molecular pharmaceutics

ARTICLE

pubs.acs.org/molecularpharmaceutics

Chemical Conjugation of the Neuropeptide Kyotorphin and Ibuprofen Enhances Brain Targeting and Analgesia

Marta M. B. Ribeiro,[†] Antónia R. T. Pinto,[‡,§] Marco M. Domingues,[†] Isa Serrano,[†] Montserrat Heras,[∥] Eduard R. Bardaji,[∥] Isaura Tavares,[‡,§] and Miguel A. Castanho*[,†]

[†]Instituto de Medicina Molecular, Faculdade de Medicina de Lisboa, Av. Professor Egas Moniz, 1649-028 Lisboa, Portugal

[‡]Instituto de Histologia e Embriologia, Faculdade de Medicina do Porto, Alameda Professor Hernâni Monteiro, 4200-319 Porto, Portugal

[§]Instituto de Biologia Celular e Molecular, Rua Campo Alegre, 4150-180 Porto, Portugal

[∥]Laboratori d'Innovació en Processos i Productes de Síntesi Orgànica (LIPPSO), Departament de Química, Universitat de Girona, Campus Montilivi, 17071 Girona, Spain

Supporting Information

ABSTRACT: The pharmaceutical potential of natural analgesic peptides is mainly hampered by their inability to cross the blood−brain barrier, BBB. Increasing peptide−cell membrane affinity through drug design is a promising strategy to overcome this limitation. To address this challenge, we grafted ibuprofen (IBP), a nonsteroidal anti-inflammatory drug, to kyotorphin (L-Tyr-L-Arg, KTP), an analgesic neuropeptide unable to cross BBB. Two new KTP derivatives, IBP-KTP (IbKTP-OH) and IBP-KTP-amide (IbKTP-NH_2), were synthesized and characterized for membrane interaction, analgesic activity and mechanism of action. Ibuprofen enhanced peptide−membrane interaction, endowing a specificity for anionic fluid bilayers. A direct correlation between anionic lipid affinity and analgesic effect was established, IbKTP-NH_2 being the most potent analgesic (from 25 μmol·kg^{-1}). In vitro, IbKTP-NH_2 caused the biggest shift in the membrane surface charge of BBB endothelial cells, as quantified using zeta-potential dynamic light scattering. Our results suggest that IbKTP-NH_2 crosses the BBB and acts by activating both opioid dependent and independent pathways.

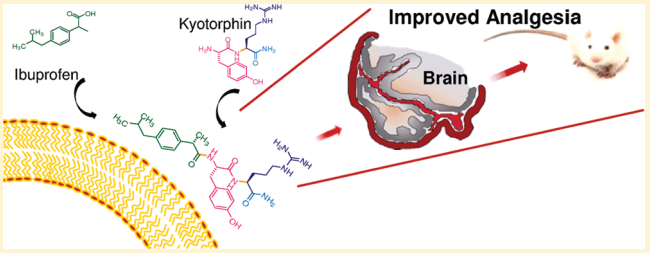

KEYWORDS: kyotorphin, ibuprofen, analgesia, blood−brain barrier, peptide−membrane interaction, lipophilicity

1. INTRODUCTION

Kyotorphin (KTP) is an endogenous dipeptide (L-Tyr-L-Arg) first isolated from bovine brain[1] and subsequently found in the brains of other mammals, including humans.[2] It acts as a neurotransmitter/neuromodulator in nociceptive responses in the central nervous system, having an analgesic potency approximately 4.2-fold higher than endogenous opioid peptides.[3] Other activities have been proposed such as inhibiting cell proliferation and antihibernating regulation.[4] The mechanism of action of this multifunctional peptide remains, however, unknown. There is evidence suggesting that KTP does not bind to opioid receptors, raising the possibility of a specific receptor for KTP, not yet identified. Whatever the mechanism, a release of Met-encephalin is acknowledged by all the authors.[5]

Despite its interesting properties, KTP is only active when injected directly into the brain. When systemically administered, it only shows brief activity and at a high dose of 200 mg·kg^{-1}.[6] This limited capacity to cross the BBB, mainly related to both insufficient lipophilicity and susceptibility to various lytic enzymes, confines KTP pharmacological applications. A logical strategy to target KTP to the brain is the chemical modification of KTP into lipophilic analogues.[6,7] Accordingly, a direct correlation between improved interaction with lipid bilayers and analgesic activity for KTP derivatives has been reported.[8]

Recently, we discovered and characterized a new kyotorphin derivative, KTP-amide.[9] This new peptide, KTP-NH_2, is analgesic upon systemic administration to animal models, which, combined with an inhibition of nociceptive responses of spinal neurons, suggests a central effect of the drug.[9] Although KTP-NH_2 analgesia is inhibited by naloxone administration (either ip or i.t.), direct binding of KTP-NH_2 to opioid receptors is nearly absent, similarly to the original, nonamidated, dipeptide. Also, amidation of KTP appeared to enhance peptide partition to biomembranes. Nevertheless, the peptide's reduced size and susceptibility to enzyme degradation (resulting in a high oral dose required to induce analgesia[9]) prompted us to design an improved derivative.

In the clinics, a combination of more than one analgesic is frequently used with success. As a matter of fact, the complexity

Received: June 16, 2011
Accepted: August 10, 2011
Revised: July 28, 2011
Published: August 10, 2011

dx.doi.org/10.1021/mp2003016 | *Mol. Pharmaceutics* 2011, 8, 1929–1940

of tissue injury, inflammation, signal transduction and pain pathways demands a *multitarget* strategy, attacking multiple pain sources and mechanisms altogether.[10] Herein, we propose an innovative covalent combination of kyotorphin (both amidated and nonamidated) with ibuprofen, a lipophilic nonsteroidal anti-inflammatory drug (NSAID) that is toxicologically safe, hereafter referred to as IbKTP-OH and IbKTP-NH_2 (Figure 1A, structures **5** and **7**). This construct results from both chemical reasoning (IBP renders KTP more lipophilic) and medical reasoning (a combination of painkillers of different classes). Ibuprofen is an anti-inflammatory drug (nonselectively inhibits cyclooxygenase 1 and 2) with analgesic properties: it enhances the analgesic action of anandamide in a way sensitive to cannabinoid receptors (both CB1 and CB2).[11] Only limited information exists on the brain distribution of ibuprofen: while some authors defend that it can get into the brain,[12] others reported a nearly absent permeability of BBB to IBP.[13] IBP has received much attention lately because it may be a neuroprotective agent,[12] which is believed to be related to its nitric oxide radical scavenging activities in neuronal cells. Accordingly, IBP was shown to be the only NSAID that, when taken regularly, reduced by 40% the likelihood of developing Parkinson's disease in humans.[14] These new reports gathered further evidence of BBB crossing by IBP and increase the interest on studying IBP containing compounds.

In the present work, we first used the intrinsic fluorescence of tyrosine to study the lipophilicity of IbKTP derivatives *in vitro* in lipid vesicles. The influences of membrane charge, lipid phase and sterol presence were also studied. We then moved toward an *in vivo* proof of concept of the biophysical rationale, through *in vivo* antinociception behavior analysis. Our data presented here show that an unusual chemical grafting of an analgesic peptide with ibuprofen, a nonsteroidal anti-inflammatory drug, resulted in a highly analgesic peptide. Moreover, our results suggest that a preference for anionic membranes correlates with BBB crossing. Indeed, we showed that IbKTP-NH_2 interacts with BBB endothelial cells by binding to their membranes because it partially neutralizes the membrane negative charge. Moreover, our results indicate a dual action of IbKTP-NH_2: opioid dependent and independent.

2. EXPERIMENTAL SECTION

2.1. General Synthetic Procedures. The peptides were synthesized by a standard solution peptide synthesis using benzotriazol-1-yloxytris(dimethylamino)phosphonium hexafluorophosphate (BOP) and *N*-hydroxybenzotriazole (HOBt) as coupling reagents and *N*-methylmorpholine (NMM) as a base. See Supporting Information for details of ibuprofen−kyotorphin derivative synthesis.

2.2. Characterization in Aqueous Solution. IbKTP-NH_2 (153 μM), IbKTP-OH (263 μM) and Tyr (143 μM) solutions were prepared in 10 mM 4-(2-hydroxyethyl)-1-piperazineethanesulfonic acid (HEPES) buffer, pH 7.4, 150 mM NaCl, and all assays were carried out at room temperature. Spectral characterization of KTP peptides and Tyr in aqueous solution was performed at an excitation wavelength of 275 nm, except for the acrylamide quenching experiments with excitation at 284 nm. Fluorescence quenching data were analyzed using the Stern−Volmer equation[15] (eq 1):

$$\frac{I_0}{I} = 1 + K_{SV}[Q] \quad (1)$$

(K_{SV} is the Stern−Volmer constant, which depends on the kinetic bimolecular rate constant; I is the fluorescence intensity at quencher concentration $[Q]$, and I_0 is the fluorescence intensity in the absence of quencher). See Supporting Information for details on peptides' biophysical characterization.

2.3. Lipid Preparation. Large unilamellar vesicles (LUVs) with 100 nm diameter were prepared by the extrusion method described elsewhere[16] and used as model of biological membranes. Several systems were analyzed: POPC (1-palmitoyl-2-oleoyl-*sn*-glycero-3-phosphocholine), POPC:POPG {POPC:[1-palmitoyl-2-oleoyl-*sn*-glycero-3-(phospho-*rac*-(1-glycerol))]} (80%:20%, 50%:50%), POPG, POPC:cholesterol (82%:18%, 75%:25%, 67%:33%).

2.4. Membrane Partition Studies. Membrane partition studies were performed by successive additions of a 15 mM lipid suspension to an IbKTP-NH_2 or IbKTP-OH solution, with 10 min incubation time in between additions and before each measurement. The partition coefficients, K_p, were calculated from the fit of the experimental data with eq 2,[17]

$$I = \frac{I_W + K_p\gamma_L[L]I_L}{1 + K_p\gamma_L[L]} \quad (2)$$

where I_W and I_L are the limit fluorescence intensities in aqueous solution and in lipid, respectively, γ_L is the molar volume of the lipid[18] and $[L]$ is the lipid concentration. The fraction of peptide interacting with membranes (X_L) and the fraction of light emitted by the peptide incorporated in the vesicles (f_L) were determined according to ref 18.

2.5. Localization in Lipidic Membranes. The membrane in-depth location of the Tyr residue in IbKTP derivatives was studied by differential quenching methodologies. Titration of peptides in the presence of LUVs (3 mM) was carried with successive additions of 5-doxylstearic acid (5-NS) and 16-doxylstearic acid (16-NS) (ethanolic solutions) up to 1.2 mM. The assays consisted in measuring fluorescence emission intensity (λ_{exc} = 282 nm, λ_{em} = 306 nm). Data was analyzed through the Stern−Volmer equation (eq 1). If a positive deviation was observed, data was interpreted as a quenching sphere-of-action,[19] which states the existence of a sphere of volume V centered at the fluorophore, where the quenching occurs with a determined efficiency γ and analyzed using eq 3:

$$\frac{I_0}{I} = (1 + K_{SV}[Q])\, e^{V[Q]N_A\gamma} \quad (3)$$

Regarding the positive deviation to the Stern−Volmer relationship, the Lehrer equation,[15] eq 4, was applied:

$$\frac{I_0}{I} = \frac{1 + K_{SV}[Q]}{(1 + K_{SV}[Q](1 - f_B) + f_B)} \quad (4)$$

An improved version of the method described in ref 20 was used to obtain the in-depth distribution in the bilayer of the Tyr residues of IbKTP-NH_2 and IbKTP-OH. Quencher concentration shown is relative to the effective concentration in the vesicles.

2.6. Dipole Potential Membrane Assays. Changes in the membrane dipole potential magnitude were monitored by means of fluorescence excitation spectral shifts of the dye (4-[2-[6-(dioctylamino)-2-naphthalenyl]ethenyl]-1-(3-sulfopropyl) (di-8-ANEPPS).[21] Small volumes of di-8-ANEPPS dissolved in ethanol were added to LUV and incubated overnight. Final concentrations used were 200 μM for lipids and 5 μM for di-8-ANEPPS.

A

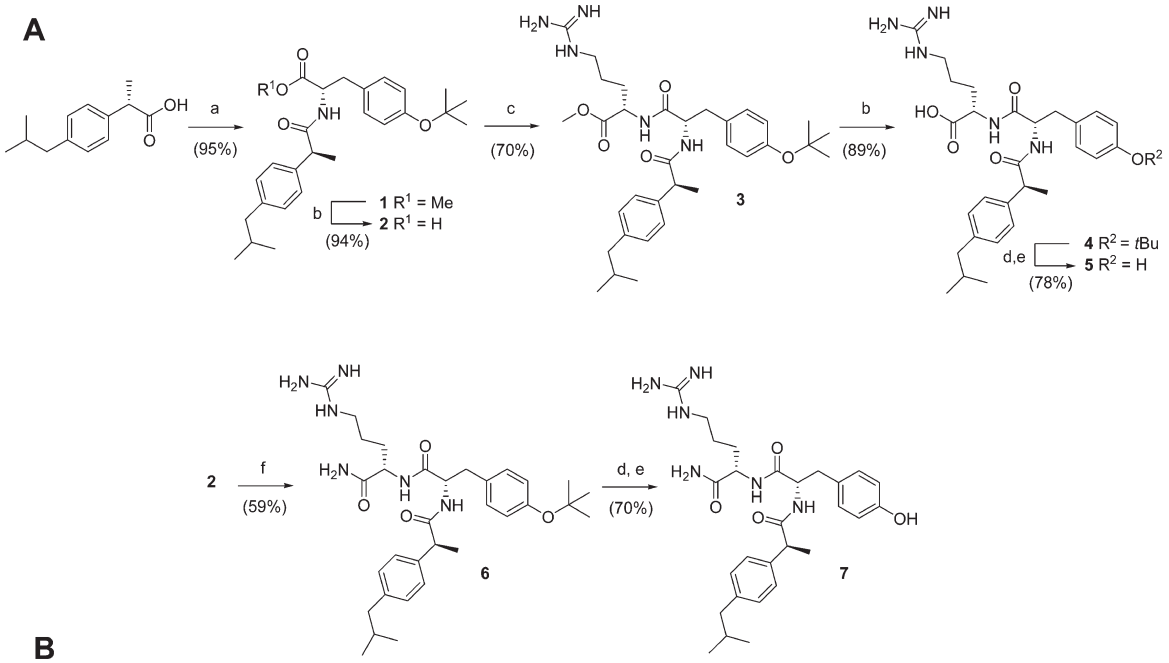

B

Entry	Coupling reagents	Temperature (ºC)	Time (h)	Compound	Yield (%)[a]	Diastereoisomeric ratio[b]
1	BOP (1 eq) NMM (3eq)	rt	24	**3**	65	62:38
2	BOP (1 eq) NMM (3 eq)	rt	24	**6**	58	58:42
3	DCC (1 eq) HOBt (1 eq) NMM (1.2 eq)	-10	24	**3**	-	-
4	BOP (1 eq) HOBt (3 eq) NMM (3 eq)	-10	24	**3**	63	77:23
5	BOP (1 eq) HOBt (3 eq) NMM (3 eq)	-30	48	**3**	60	76:24
6	BOP (1 eq) HOBt (5 eq) NMM (3 eq)	-15	21	**3**	66	85:15
7	BOP (1 eq) HOBt (6 eq) NMM (3 eq)	-15	21	**3**	70	88:12
8	BOP (1 eq) HOBt (6 eq) NMM (3 eq)	-15	21	**6**	59	87:13

[a]Isolated yields. [b]Determined by ^{1}H NMR

Figure 1. Synthesis of IbKTP derivatives: IbKTP-OH (structure **5**) and IbKTP-NH_2 (structure 7). (A) Reagents and conditions: (a) H-Tyr(tBu)-OMe·HCl (1 equiv), BOP (1 equiv), NMM (3 equiv), DMF, rt, 6 h; (b) LiOH (2.5 equiv) THF/MeOH/H_2O (1:2:2), rt, overnight; (c) H-Arg-OMe·2HCl (1 equiv), BOP (1 equiv), HOBt (6 equiv), NMM (3 equiv), DMF, −15 °C to rt, 21 h; (d) TFA/DMF (1:1), rt, 2 h; (e) HCl (1M), lyophilization, 3 times; (f) H-Arg-NH_2·2HCl (1 equiv), BOP (1 equiv), HOBt (6 equiv), NMM (3 equiv), DMF, −15 °C to rt, 21 h. (B) IbKTP derivative optimization study.

2.7. Brain Capillary Endothelial Cell (BCEC) Preparation. Confluent BCEC were 3 times washed with phosphate buffer saline (PBS) buffer followed by trypsinization. Cells were counted and diluted with PBS for final concentration of 1×10^5 cells/mL and measured for zeta-potential. See Supporting Information for details on BCEC preparation.

2.8. Human Umbilical Vein Endothelial Cell (HUVEC) Preparation. HUVEC were kindly provided by Dra. Susana C. Santos (Portugal) and cultured in complete endothelial medium. Upon reaching confluence, cells were passed onto other gelatin coated flasks and used at the sixth passage. For zeta-potential measurements, HUVEC were 3 times washed with PBS buffer followed by trypsinization. Finally, cells were counted and diluted with PBS for final concentration of 1×10^5 cells/mL.

2.9. Zeta-Potential Measurements. Measurements were conducted on a dynamic light scattering and zeta-potential equipment, equipped with a He−Ne laser (λ = 632.8 nm). The zeta-potential of the samples was determined at 25 °C using disposable zeta cells with platinum gold-coated electrodes as described in ref 22. 1-(4-(Trimethylamino)phenyl)-6-phenyl-1,3,5-hexatriene (TMA-DPH) was added for a final concentration of 54 μM and incubated for 30 min previous to measurements. IbKTP derivatives were added to the cell sample both at 200 μM and equilibrated for 15 min prior to the measurement. Each group value is an average of at least two independent measurements. The electrophoretic mobility obtained was used for the zeta-potential calculation through the Smoluchowski equation,[23]

$$\zeta = \frac{4\pi\eta\mu}{\varepsilon} \quad (5)$$

where μ represents the electrophoretic mobility, η the viscosity of the solvent and ε its dielectric constant.

2.10. Animals. The experiments were performed according to the ethical Guidelines of the International Association for the Study of Pain[24] and the European Community Council Directive (86/609/EEC). Adult male Wistar rats (Charles River, Spain) weighing 275−300 g at the beginning of experiments were used. All peptides were dissolved in saline containing 10% of dimethyl sulfoxide (DMSO). Intrathecal catheters were implanted as described before.[9] On the experiment day, naloxone was i.t. injected (10 μL; 5 mg·mL^{-1}) followed, 10 min later, by the ip administration of either of the peptides.

2.11. Acute Pain Experiments. The effect of the peptides at 25 μmol, 50 μmol and 96 μmol·kg^{-1} bw was evaluated by the tail-flick and hot-plate tests as described elsewhere.[9] See Supporting Information for details on acute pain experiment methodology.

2.12. Inflammatory Pain Experiments. The formalin test was performed as described previously.[9,25] Data is presented as the number of jerks/flinches (named here as paw-jerks) and focused-pain related activity of the injected hind paw in 12 successive periods of 5 min each.

2.13. Immunostaining for Fos. Two hours after formalin injection, the time point of maximal expression of the proto-oncogene c-fos,[26] animals were sacrificed for the analysis of c-fos activation as previously described.[9] Mean numbers of Fos-immunoreactive neurons per section were calculated. See Supporting Information for details on Fos immunostaining.

2.14. Statistical Analyses. Data are represented as the groups' mean + SEM (standard error of the mean). The significance of differences in each group was analyzed with Friedman's test followed by Dunn's multiple comparison test. The significance of differences for each dose and time point compared with the KTP-treated controls was analyzed with the nonparametric two-tailed Mann−Whitney test. All statistical analyses were calculated with Prism software (GraphPad Software, version 5).

3. RESULTS

3.1. IbKTP-NH$_2$ and IbKTP-OH Synthesis. Nonamidated and amidated ibuprofen-kyotorphin derivatives, IbKTP-OH (**5**) and IbKTP-NH$_2$ (**7**), have been prepared following standard solution peptide synthesis as illustrated in Figure 1A. Coupling between optically pure (*S*)-ibuprofen and protected L-tyrosine was mediated by BOP, 1 equiv in the presence of NMM (3 equiv)[27] and afforded compound **1** with good yield. Subsequent saponification of methyl ester **1** with LiOH[28] provided the common intermediate **2** also with good yield. Initially, compound **2** and L-arginine methyl ester were coupled using the same reaction conditions. Disappointingly, dipeptide **3** was obtained as a diastereoisomeric mixture (Figure 1B, entry 1). A similar result was obtained for compound **6** when compound **2** was coupled with L-arginine amide (Figure 1B, entry 2). ^{1}H NMR (nuclear magnetic resonance) spectra of compounds **3** and **6** recorded in DMSO-d_6 showed split signals. Compared to their precursors, the ^{1}H NMR spectrum of dipeptide **3** showed almost all protons split as two sets of signals (Figure S1 in the Supporting Information). In order to prove racemization or a possible conformational equilibrium, an NMR study was undertaken. The ^{1}H NMR of compound **3** did not exhibit line broadening from 25 to 85 °C in DMSO-d_6, which would be expected if a slow conformational equilibrium occurred (Figure S2 in the Supporting Information). An optimization study was conducted for the synthesis of compound **3** in order to reduce the racemization degree. The different variables (coupling reagent equivalents, temperature and reaction time) were systematically changed (Figure 1B). No reaction took place when dicyclohexylcarbodiimide (DCC) was employed as a coupling reagent in the presence of the commonly used racemization suppressant agent HOBt[29] (Figure 1B, entry 3). However, racemization could be significantly diminished when BOP was used as coupling reagent and a large amount of HOBt[30] was added to the reaction mixture (Figure 1B, entries 4−7) at low temperature. An increase of the amount of HOBt led to a decrease of racemization until an acceptable diastereoisomeric ratio of 88:12 (Figure 1B, entry 7). Dipeptide **6** was also obtained in a similar racemization degree using the above coupling reaction conditions. In all cases, diastereoisomeric ratio was determined by NMR integration of the aromatic protons signals at 6.7 and 6.85 ppm respectively (Figures S3 and S4 in the Supporting Information). The IbKTP-OH derivative **5** was obtained after methyl ester saponification of dipeptide **3** followed by treatment of the resulting free acid **4** with trifluoroacetic acid (TFA) to remove *tert*-butyl protecting group. Dipeptide **6** was converted into IbKTP-NH$_2$ derivative **7** by *tert*-butyl removal with TFA (Figure 1A). Final compounds **5** and **7** were dissolved in 1 M HCl and lyophilized. This last step was repeated three times in order to obtain derivatives **5** and **7** as hydrochloride salts instead of a trifluoroacetic salt for subsequent administration to model animals.

3.2. Characterization in Aqueous Solution. KTP has one Tyr residue, which allows structural characterization by fluorescence spectroscopy. In aqueous solution and under physiological pH and ionic strength conditions, absorption and emission spectra profiles of both derivatives, IbKTP-NH$_2$ (153 μM) and

IbKTP-OH (263 μM), are similar to those of free tyrosine (Figure 2A). With an absorption maximum at 273 nm and an emission maximum at 302 nm, a small deviation on the maximal absorption wavelength in comparison to Tyr is observed which is probably related to the additional effect of IBP spectrum ($\lambda_{abs,max}$ = 264 nm and $\lambda_{em,max}$ = 298 nm).

No red-edge excitation-shift effects were detected. The fluorescence quantum yield (ϕ) in aqueous solution at 23 °C is 0.054 and 0.069 for IbKTP-NH_2 and IbKTP-OH, respectively, which is lower than that of free Tyr (ϕ = 0.140[31]). The fluorescence of an aromatic amino acid side chain can be quenched by the peptide backbone as a consequence of a charge transfer between the excited chromophore (phenol ring), acting as a donor, and electrophilic units in the amino acid backbone, acting as an acceptor.[31] Ross et al.[32] also observed that if the phenol side chain is shielded from solvent and the local environment contains no proton acceptors, then many intra- and intermolecular interactions result in a reduction of the quantum yield. Moreover, the fact that IbKTP-NH_2 reveals the lowest ϕ is in agreement with studies that showed amide group as a quencher of tyrosine fluorescence.[33] These results are in conformity with results observed for other KTP derivatives.[7,8] The study of intermolecular quenching can be used to evaluate the accessibility of fluorophore to quenchers whose location is known.[19] Linear Stern−Volmer plots for the fluorescence quenching of the peptide by the hydrophilic molecule acrylamide, for instance, are evidence that Tyr residues are equally exposed to the surrounding aqueous medium (Figure S5A in the Supporting Information), which rules out the possibility of compact aggregates. Fitting the experimental data to Stern−Volmer equation (eq 1), K_{SV} was calculated to be 9.9 and 14.8 M^{-1} for IbKTP-NH_2 and IbKTP-OH, respectively. The slightly lower value observed for IbKTP-NH_2 may be related to the addition of the amide group to the Arg residue, resulting in a conformational alteration that restrains the accessibility of acrylamide to the Tyr residue. To further evaluate possible changes in the supramolecular structure of KTP derivatives, namely, aggregation, the fluorescence quantum yield dependence on peptide concentration was studied. No significant deviations from linearity were observed in a fluorescence intensity vs concentration plot, i.e., there is no dependence of quantum yield on concentration (Figure S5B in the Supporting Information). It may then be concluded that the dominant forms of the derivatized dipeptides are monomers or small loose oligomers.

3.3. Extent of Partition into Fluid Lipid Bilayers. We started by evaluating the partition of both peptides toward liquid-crystal (fluid) bilayers, constituted by zwitterionic POPC and anionic POPG in different proportions, to model human cells' membranes and appraise the effect of anionic lipids. Titration of aqueous suspensions of IbKTP-NH_2 with LUVs led to an increase in the fluorescence quantum yield, indicating that the peptide is interacting with the membranes (Figure 2B). This change in fluorescence intensity is related to the partition constant, K_p, by eq 2. When titrated with POPC, K_p is $(0.19 \pm 0.06) \times 10^3$. There is a clear effect of charge on the partition of peptide toward the membrane: K_p increases exponentially with the molar fraction content of the negatively charged lipid POPG in the POPC bilayer (Figure 2D,G), reaching a maximum when the membrane is 100% POPG [$(8.1 \pm 0.8) \times 10^3$]. In the case in which the IBP moiety is absent (KTP-NH_2), it is difficult to define a specific pattern of interaction dependent on the anionic lipidic composition, with K_p varying in a small range of values (Table S1 in the Supporting Information). Interestingly, the grafting of ibuprofen favored the selective interaction toward anionic vesicles. The strong influence of the negative charge of lipids is also noticed on the fraction of peptide partitioned to the membrane at a certain fixed lipid concentration: X_L[18] (Figure 2G). While for KTP-NH_2 X_L values at 3 mM lipid are between 0.79 and 0.87 irrespective of POPG proportion in the vesicles (Table S1 in the Supporting Information), in the case of IbKTP-NH_2, they increase markedly with anionic charge in the membranes.

The original endogenous nonamidated kyotorphin molecule, KTP-OH, partition at physiologic conditions has been described as reduced, with preference for cholesterol (chol) containing membranes.[7] When derivatized with IBP, an increase in the interaction of the dipeptide with the membrane was observed, accompanied by a change of preference toward fluid phase lipids (Figure 2C). The highest K_p reaches $(1.8 \pm 0.5) \times 10^3$ for an equimolar mixture of POPC and POPG (Figure 2C,G). Thus, both hydrophobic and electrostatic interactions seem to contribute for IbKTP-OH partition toward the membrane.

3.4. Extend of Partition into Cholesterol-Containing Bilayers. POPC vesicles containing 18% and 33% molar cholesterol were used to study the partition of peptides toward liquid-ordered membranes.[34] For IbKTP-NH_2, K_p decreased with an increase in the cholesterol content in the membranes (Figure 2B,G). At variance, improved interaction was observed for IbKTP-OH, when compared to POPC vesicles (Figure 2C,G). These IbKTP-OH results are in agreement with similar data for KTP-OH.[7]

3.5. Localization of Peptides in Lipid Bilayers. In-depth location of Tyr residue in kyotorphin peptides was carried out by means of differential fluorescence quenching using two lipophilic doxyl stearic acids (5-NS and 16-NS). The closer the Tyr residues are to the quencher group, the more efficient is the quenching. Considering their distributions, 5-NS probes the bilayer interface whereas 16-NS probes its core. By combining the results from both quenchers, one can estimate the membrane depth distribution of the fluorophore.

5-NS was the most efficient quencher of the fluorescence for both peptides, indicating a preferred location near the lipid bilayer interface (Figure 2E,F). When titrated with 5-NS, IbKTP-NH_2 Stern−Volmer plots show a positive deviation from linearity, which may be ascribed to simultaneous static and dynamic quenching effects.[19] A negative deviation from linearity in the Stern−Volmer plot was observed for IbKTP-OH, indicating the presence of heterogeneous subpopulations of the fluorophore relative to the accessibility to the quenchers (Figure 2E). Equation 3 and eq 4 were applied to data to obtain Stern−Volmer constants, K_{SV}, and the fraction of fluorophore accessible to the quencher, f_B. The f_B values can be compared to the fraction of fluorescence intensity originating from the peptide in the lipid, f_L (Figure 2G and Table S1 in the Supporting Information[18]). Brownian dynamics simulation of the quenchers in membrane[20] allowed the in-depth distribution of Tyr residues to be obtained taking into account the possibility of static quenching by using a sphere-of-action methodology.[19] All peptides showed a superficial localization (Figure 2F).

3.6. Effect of IbKTP Derivatives on Brain Endothelial Cell Membrane. In order to underpin the effect of each IbKTP derivative on the membrane of cells constituting the BBB, we measured membrane zeta-potential, ζ, of primary bovine cultures of BCEC in the presence of each IbKTP derivative (Figure 3). Although endothelial cell membranes are generally known as displaying a negative charge,[35] a direct quantification of their

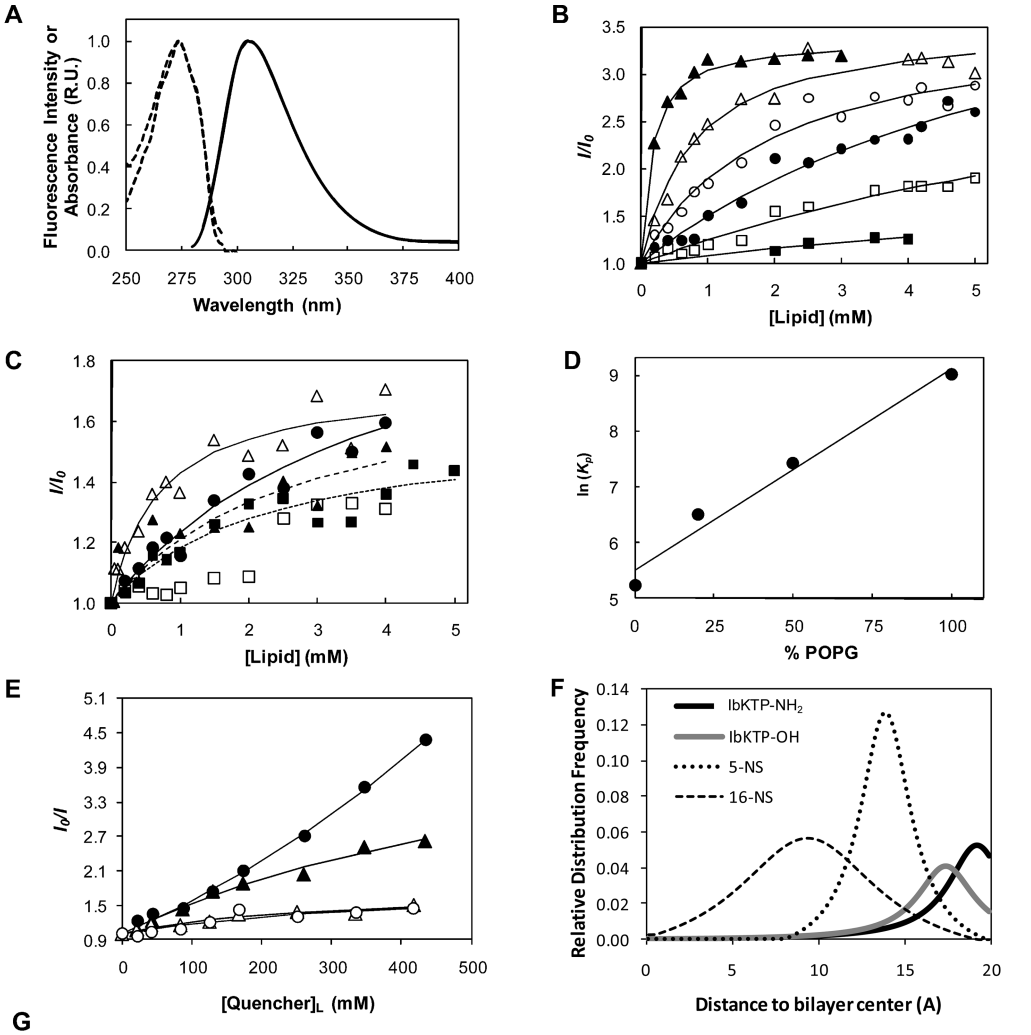

G

Lipidic mixture	Peptide	K_p (x10^3)	X_L	f_L	$f_{B,5-NS}$	$K_{SV,5-NS}$ (M^{-1})	$f_{B,16-NS}$	$K_{SV,16-NS}$ (M^{-1})
POPG	IbKTP-NH$_2$	8.1±0.8	0.95±0.18	0.98±0.18	1	5.1±0.1	0.71±0.11	3.5±1.2
	IbKTP-OH	0.48±0.32	0.52±0.53	0.66±0.57	0.86±0.08	3.7±0.8	0.32±0.17	3.1±3.4
POPC:POPG (50%)	IbKTP-NH$_2$	1.7±0.3	0.79±0.23	0.93±0.24	1*	4.8±0.6*	-	-
	IbKTP-OH	1.8±0.5	0.81±0.38	0.88±0.39	1*	3.5±0.1	0.75±0.38	1.2±0.9
POPC:POPG (20%)	IbKTP-NH$_2$	0.68±0.12	0.61±0.17	0.85±0.20	0.96±0.10	5.2±0.9	0.57±0.04	4.7±0.8
	IbKTP-OH	-	-	-	0.96±0.03	5.2±0.5	0.31±0.03	10.1±3.0
POPC	IbKTP-NH$_2$	0.19±0.06	0.30±0.13	0.68±0.18	0.99±0.22	4.3±2.1	0.47±0.14	4.7±3.2
	IbKTP-OH	0.33±0.12	0.43±0.23	0.62±0.25	0.82±0.03	7.4±1.0	0.43±0.05	7.2±2.4
POPC:Chol (18%)	IbKTP-NH$_2$	0.12±0.06	0.21±0.13	0.51±0.18	-	-	0.54±0.04	3.9±0.6
	IbKTP-OH	-	-	-	-	-	0.60±0.25	1.9±1.3
POPC:Chol (33%)	IbKTP-NH$_2$	0.09±0.16	0.18±0.35	0.32±0.39	-	-	0.42±0.10	2.9±1.3
	IbKTP-OH	0.57±0.21	0.57±0.33	0.68±0.36	0.86±0.04	5.7±0.8	0.48±0.18	2.1±1.3

*data was fitted using Equation 3

Figure 2. Biophysical characterization of IbKTP derivatives in aqueous solution and in interaction with membranes. (A) Normalized absorption and emission (λ_{exc} = 273 nm) spectra of IbKTP-NH$_2$ (Dotted line) and IbKTP-OH (Dashed line) in aqueous solution. (B-D) Partition of IbKTP derivatives with vesicles. Titration of IbKTP-NH$_2$ (B) and IbKTP-OH (C) with concentrated LUV suspension. Lines represent fittings of eq 2[17] to the data. POPG (▲); POPC:POPG (50%) (△); POPC:POPG (20%) (○); POPC (●); POPC:Chol (18%) (□); POPC:Chol (33%) (■). (D) K_p (logarithmic scale) of IbKTP-NH$_2$ dependence on POPC:POPG molar ratio. (E, F) IbKTP derivatives localization in the membrane. (E) Stern−Volmer plot of the fluorescence *quenching* of IbKTP-NH$_2$ (●; ○) and IbKTP-OH (▲; △) by 5-NS (●; ▲) and 16-NS (○; △). Solid lines represent fittings of eqs 3 and 4 to the experimental data. (F) In-depth distribution of Tyr residues of IbKTP-NH$_2$ and IbKTP-OH in lipid bilayers is obtained from the data in (E) upon application of a differential *quenching* method.[20] The fluorophore distribution in the membrane is given as probability density function relative to the distance to the bilayer center. (G) Parameters obtained for the partition and quenching of the fluorescence of IbKTP-NH$_2$ and IbKTP-OH by the lipophilic probes 5-NS and 16-NS in membranes using different lipidic mixtures. Assays performed at room temperature in a 10 mM HEPES buffer, pH 7.4, containing 150 mM NaCl. Quenching experiments performed at a total lipidic concentration of 3 mM. K_p was determined by fitting eq 2 to the data.

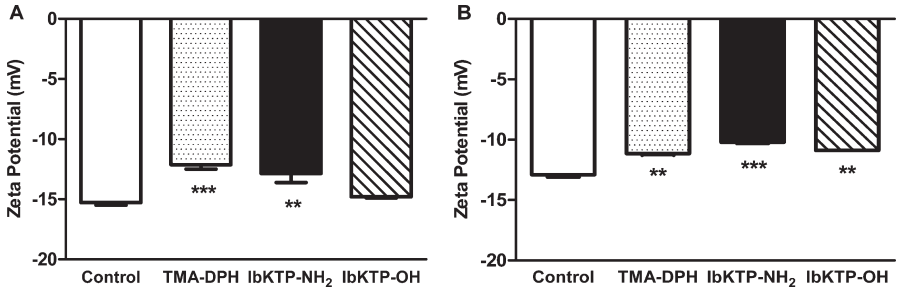

Figure 3. Zeta-potential of primary endothelial cells in the presence of IbKTP derivatives. BCEC (A) and HUVEC (B) at 1×10^5 cells/mL (PBS buffer) were incubated with TMA-DPH (54 μM), IbKTP-NH_2 and IbKTP-OH (both at 200 μM) at 25 °C, and zeta potential was measured. Data shown as means ± SEM; each group value is an average of at least two independent measurements. $^{**}P < 0.01$; $^{***}P < 0.001$ versus BCEC or HUVEC control; one-way ANOVA, Bonferroni's multiple comparison test.

membrane charge has never been performed to the best of our knowledge. BCEC membrane surface charge through zeta-potential was revealed to be highly negative, $\zeta = -15.28 \pm 0.582$ mV. TMA-DPH, a cationic probe of membrane dynamics in living cells with a cationic charge (+1), was used as a positive control because it intercalates at the level of hydrophilic head groups of membrane phospholipids and neutralizes the anionic charges of lipids of the outer layer of the cytoplasmatic membrane. TMA-DPH, as expected, caused an increase in the zeta value toward neutralization ($\zeta = -12.13 \pm 0.490$ mV) (Figure 3A). The effect of IbKTP-NH_2 and IbKTP-OH on BCEC membrane surface charge was also measured. From these, only IbKTP-NH_2 significantly led to a shift in the zeta-potential of the BCEC cell membrane, toward neutralization ($\zeta = -12.85 \pm 0.492$ mV, Figure 3B). This selectivity to BBB cell membranes, observed for IbKTP-NH_2 but not for IbKTP-OH, may be the basis of different BBB-crossing potential between the two peptides. To further evaluate if this interaction profile applies to all endothelial cells, we took HUVEC and performed the same experiments. The zeta-potential of HUVEC ($\zeta = -12.89 \pm 0.564$ mV) is significantly more positive than that of BCEC (Figure 3B). Unlike the zeta-potential of BCEC, the zeta-potential of HUVEC is affected by both IbKTP-NH_2 ($\zeta = -10.2 \pm 0.571$ mV) and IbKTP-OH ($\zeta = -11.3 \pm 0.482$ mV) (Figure 3B). These results correlate well with the results obtained with membrane vesicles, which revealed IbKTP-NH_2 to be very lipophilic, mainly when anionic membranes are involved. Zeta-potential results show that grafting KTP with IBP (IbKTP-OH) grants increased interaction with anionic surface endothelial cells, and additional amidation (IbKTP-NH_2) allows a certain degree of selectivity to BCECs.

3.7. IbKTP-NH_2 and IbKTP-OH Analgesia in Acute Pain Models. The peptides' analgesic effect was evaluated following ip administration to male Wistar rats. Acute pain models using thermal stimuli were applied: tail flick and hot plate tests.[36] The doses of both peptides tested were based on previous results for KTP-NH_2.[9] Briefly, we started with the intermediate dose of KTP-NH_2 that was efficient in all pain models tested (32.3 mg·kg^{-1} = 96 μmol·kg^{-1}). For IbKTP-NH_2, 50 μmol·kg^{-1} was used so that the test cutoff limits were not reached. Not only did IbKTP-NH_2 show a remarkable analgesic efficacy—from 25 μmol·kg^{-1} bw ($P = 0.0032$, tail flick; $P = 0.0005$, hot plate, Friedman test)—but its potency was also strikingly higher than that of the combined injection of KTP-NH_2 and ibuprofen (Figure 4A,B). In fact, linking IBP to KTP-NH_2 increased by 2-fold the analgesic efficacy in relation to the control IBP + KTP-NH_2 mixture. The analgesic effects were dose-dependent, starting at 15 min and lasting at least for 45 min.

The covalent addition of ibuprofen grants KTP-OH analgesic properties, following systemic administration. IbKTP-OH provoked a long-lasting analgesia at a dose of 96 μmol·kg^{-1} bw as revealed by the hot plate test (Figure 4D). However, the tail flick method did not reveal antinociception for IbKTP-OH (Figure 4C). Mechanistically, tail flick is considered a spinal reflex, while reactions to hot plate are related to supraspinal modulation[36] and are thus more reliable. As in the case of IbKTP-NH_2, IbKTP-OH activity was revealed to be higher than that of the control (IBP + KTP-OH), confirming a specific action for the "tandem chimeric" molecule.

Hydrophobization of both KTP-NH_2 and KTP-OH resulted in analgesic action following systemic administration, which is compatible with BBB crossing. Comparatively, IbKTP-NH_2 is the most active compound, about 3.5 times more effective than IbKTP-OH. At this point, and considering the 3R policy on animal experimentation, we selected the most promising peptide, IbKTP-NH_2, to continue the studies with model animals.

3.8. Effect of IbKTP-NH_2 in a Model of Inflammatory Pain. In order to increase IbKTP-NH_2 pharmacological relevance, we proceeded to investigate its effect in a model of sustained pain, the formalin test, which encompasses two pain phases: acute ($t < 10$ min) and inflammatory ($t > 10$ min),[25] thus being a model with translational value.[36] Moreover, it consists of a chemical stimulus, thus broadening the application range of the drug under study. Based on the time course of the effects of the drug at the acute pain tests, IbKTP-NH_2 was ip administered 10 min before formalin at the dose of 5 μmol·kg^{-1} bw. Unlike KTP-OH (used as a control due to structural similarities and inability to cross the BBB[9]), IbKTP-NH_2 reverted the typical nociception pattern at the chronic pain phase regarding focused pain-related activity and paw-jerks (Figure 5A,B). On the other side, animals injected with KTP-OH showed a pattern of behavioral responses similar to that of animals injected only with formalin.[37] Fos is a neuronal marker of nociceptive activation of spinal neurons.[26] The nociceptive activation of spinal dorsal horn neurons, laminae I—VI, induced by formalin administration was assessed by immunodetection of the Fos protein.

Animals injected with IbKTP-NH_2 showed a decrease in the number of Fos-immunoreactive neurons at the deep dorsal horn layers (Figure 5C). This constitutes evidence on the central analgesic consequences of this new peptide.

3.9. IbKTP-NH_2 Mechanism of Action. Whether kyotorphin is an opioid molecule or not has been a controversial matter of debate since its discovery. A specific KTP receptor has not been identified, and the activity of KTP-OH and KTP-NH_2 is completely

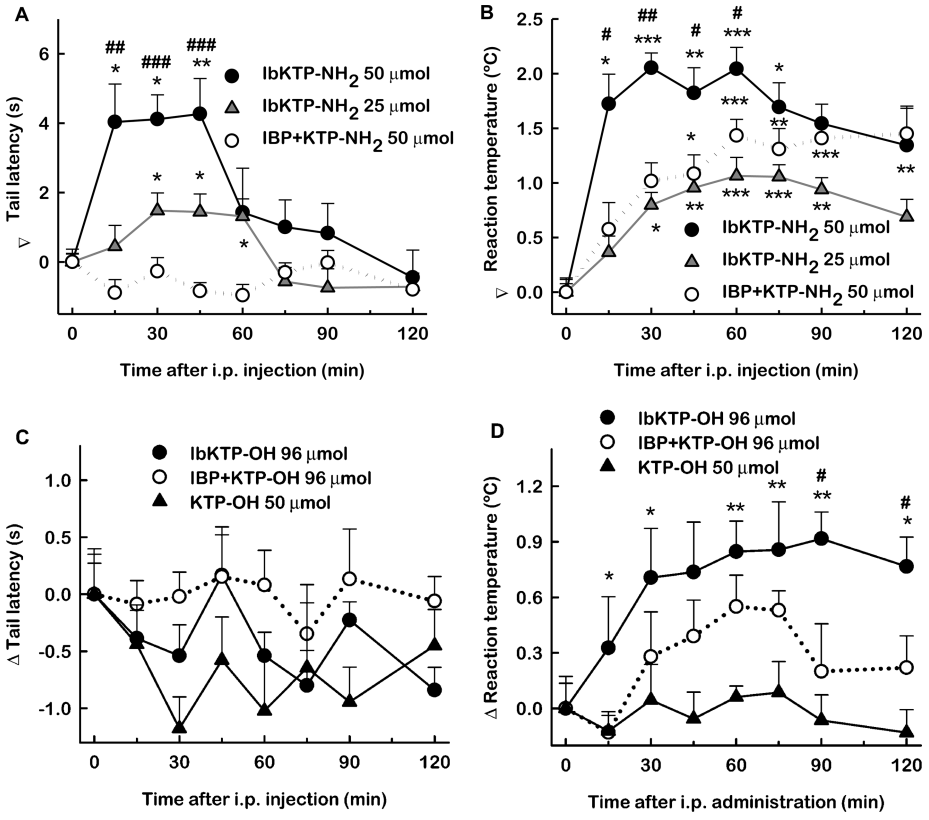

Figure 4. Analgesic action of IbKTP derivatives. Inhibition of acute nociceptive responses in the tail flick (A, C) and hot plate (B, D) tests following systemic administration of IbKTP derivatives. Results expressed as the variation of the behavioral responses at each evaluation time point in relation to baseline values (time 0) obtained immediately before injection. Doses represented for kg bw. In all experiments, $n \geq 6$. $^{*}P < 0.05$; $^{**}P < 0.01$; $^{***}P < 0.001$ versus basal response, Friedman test, and $^{\#}P < 0.05$, $^{\#\#}P < 0.01$, $^{\#\#\#}P < 0.001$ versus IBP + KTP treated controls, Mann−Whitney test. Mean + SEM for all groups.

abolished by naloxone administration, which is an unspecific opioid receptor antagonist.[9] However, direct binding between each peptide and opioid receptors is rather weak.[9,38]

The effect of central naloxone administration (i.t., 10 μL, 5 mg·mL^{-1}) over the analgesic efficacy of IbKTP-NH$_2$ (50 μmol·kg^{-1}) was evaluated to assess the involvement of opioid pathways in its analgesic mode of action. Naloxone injection significantly decreased IbKTP-NH$_2$ analgesia in the hot plate test. However, unlike KTP-NH$_2$,[9] the IbKTP-NH$_2$ antinociceptive effect was not completely inhibited by naloxone (Figure 6). This indicates that for this derivative, in addition to an opioid-dependent mode of action, there seems to be an opioid-independent mechanism. The combination of both results in a peptide with enhanced analgesic activity. It is worth stressing that we observed increased partition of IbKTP-NH$_2$ to lipid membranes as a result of IBP grafting to KTP-NH$_2$ with a preference for liquid-crystal anionic membranes. Morphine, on the other hand, is known to prefer rigid raftlike domains in the membrane, where opioid receptors tend to concentrate.[39]

To further shed light on the differences on the molecular basis of action between opioids and IbKTP-NH$_2$, we compared the membranotropic effect of morphine and IbKTP-NH$_2$. Since morphine does not display environment-sensitive intrinsic fluorescent characteristics, we used di-8-ANEPPS (4-[2-[6-(dioctylamino)-2-naphthalenyl]ethenyl]-1-(3-sulfopropyl)pyridinium) as a polarity-sensitive probe for assessing IbKTP-NH$_2$ and morphine interaction with the membrane. Binding and insertion of molecules in the membrane may change the membrane dipole potential, which can be monitored by spectral shifts of the fluorescence dye di-8-ANEPPS.[40] Fluorescence intensity difference spectra of di-8-ANEPPS when IbKTP-NH$_2$ is used are in agreement with partition data for this molecule (Figure 2B,D): the presented spectral red shifts indicate decrease in the dipole potential, and this perturbation increases with the anionic charge in the membrane (Figure 7A). As to morphine, no significant spectral shifts were observed except for cholesterol-containing bilayers (Figure 7B). The highest shift was recovered for POPC:chol (18%), in agreement with the Sargent−Schwyzer hypothesis[41] since opioid receptors are located in cholesterol-rich domains of membranes.[39] Moreover, morphine caused a blue shift effect as a result of an increase in the membrane dipole potential. This potential is originated from the alignment of dipolar residues of lipids (polar head groups and glycerol-ester regions) and oriented water molecules hydrating the outer surface of the membrane.[21]

The distinctive preference of IbKTP-NH$_2$ and morphine for POPC:POPG and POPC:Chol, respectively, points to different molecular targets and may explain why naloxone does not completely abolish the analgesic effect of IbKTP-NH$_2$.

4. DISCUSSION

Derivatizing peptides in order to improve their properties is a common approach, whether to avoid enzyme degradation, enable

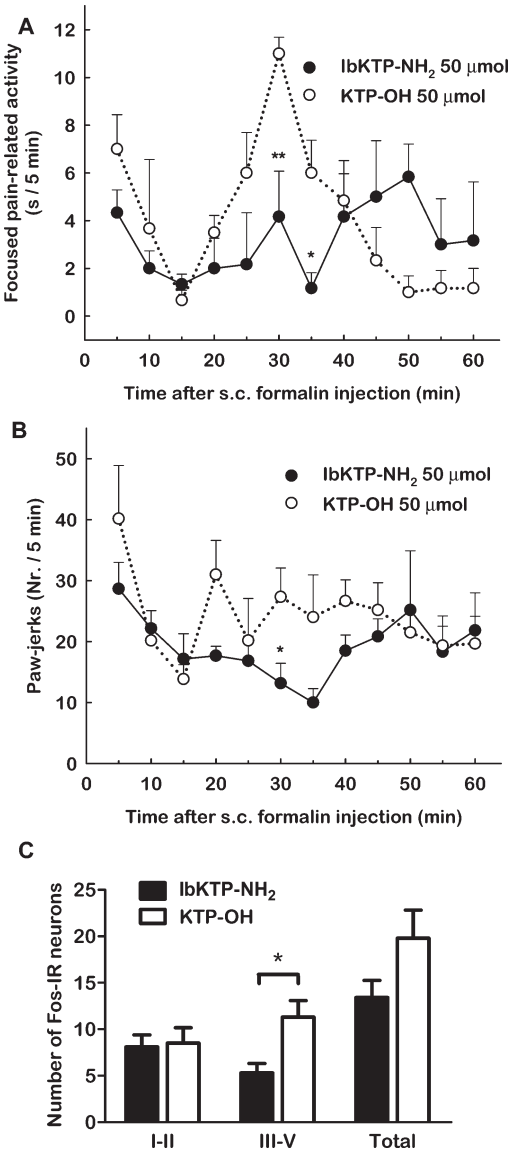

Figure 5. Analgesic profile of IbKTP-NH_2 in formalin inflammatory pain model. Time spent in focused pain-related activity (A) and number of paw-jerks (B) in 5 min time periods. The analgesic effects of an ip injection of IbKTP-NH_2 10 min before formalin injection were detected in the inflammatory phase (t > 10 min). Doses represented for kg bw. In all experiments $n \geq 6$. $^{*}P < 0.05$; $^{**}P < 0.01$ versus KTP-OH treated controls, Mann−Whitney test. Mean + SEM for all groups. (C) In formalin-injected rats, nociceptive activation of spinal neurons induced by formalin was inhibited by IbKTP-NH_2, as indicated by the lower number of Fos-immunoreactive neurons at laminae III−V at the spinal dorsal horn. $^{*}P < 0.05$, unpaired t test. Mean ± SEM for all groups.

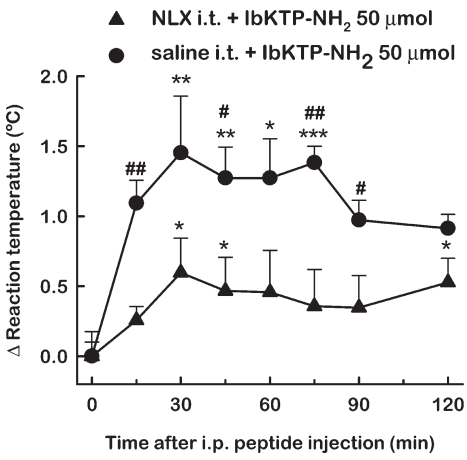

Figure 6. Opioid related mechanism of action of IbKTP-NH_2. A partial reversal of IbKTP-NH_2 induced analgesia occurred after i.t. administration of naloxone (NLX, 5 mg·kg^{-1}) in the hot plate test. Results expressed as the variation of the behavioral responses at each evaluation time point in relation to baseline values (time 0) obtained immediately before injection. In all experiments $n \geq 6$. $^{*}P < 0.05$; $^{**}P < 0.01$; $^{***}P < 0.001$ versus basal response, Friedman test, and $^{\#\#}P < 0.01$, $^{\#\#\#}P < 0.001$ versus NLX + IbKTP-NH_2 treated animals, Mann−Whitney test. Mean + SEM for all groups.

oral availability or increase biodistribution, for instance. In the specific case of brain-targeted molecules, being able to cross the blood−brain barrier is the most common quest. In this study, we tried to enhance kyotorphin analgesic properties by linking it to ibuprofen: a well-known lipophilic anti-inflammatory and analgesic drug whose ability to cross the BBB is still unclear. The influence of ibuprofen addition on the dipeptide activity was assessed at different levels: in vitro with membrane model systems and primary brain and umbilical cells, and in vivo with model animals. The absence of red-edge excitation shift, linear Stern−Volmer plots and linear dependence of fluorescence intensity with peptide concentration confirmed that IbKTP-NH_2 and IbKTP-OH do not form compact aggregates in solution, a fundamental feature when aiming a pharmacological application.

Overall, derivatization with ibuprofen largely increased partition and insertion in lipid membranes, with a clear affinity of the peptides for anionic fluid phase membranes. While the original peptide, KTP, preferred cholesterol rich membranes, IbKTP-OH displayed the highest K_p for POPC:POPG (50%:50%). In contrast, IbKTP-NH_2−membrane interaction increased exponentially with the molar fraction content of the negatively charged lipid POPG. Thus, electrostatic attraction plays a fundamental role in the binding of IbKTP-NH_2 to model membranes, in a similar way as observed for encephalin peptides.[43]

The zeta-potential measurements of BCEC and HUVEC in the presence of IbKTP-NH_2 and IbKTP-OH revealed a preference of IbKTP-NH_2 for BBB cells. Compared to HUVEC, BCEC display a more negative membrane charge, which may explain the preference of more cationic peptides to interact with and cross the BBB.[44] Therefore, we observed a preference of BCEC for IbKTP-NH_2 [positively charged (+1) at variance with IbKTP-OH, with a net neutral charge at plasma pH], which showed to be the more analgesic compound. Thus, there is an agreement between the model membrane results and the cells results. Although human endothelial cells are mainly constituted by phosphatidylcholine with smaller quantities of anionic phosphatidylserine (PS), Yeung and collaborators[45] observed that the negative charge associated with the presence of PS directed proteins with moderately positive charge to the endocytic pathway, one of the major mechanisms of absorption of peptides at the BBB level, and this is in accordance with the results reported here.

Concomitantly with biophysical results, which revealed IbKTP-NH_2 as the peptide with highest affinity to model and BCEC membranes, in vivo antinociception evaluation also revealed that this is the most effective analgesic compound. For this reason, only IbKTP-NH_2 was further studied. Insertion into the lipid matrix

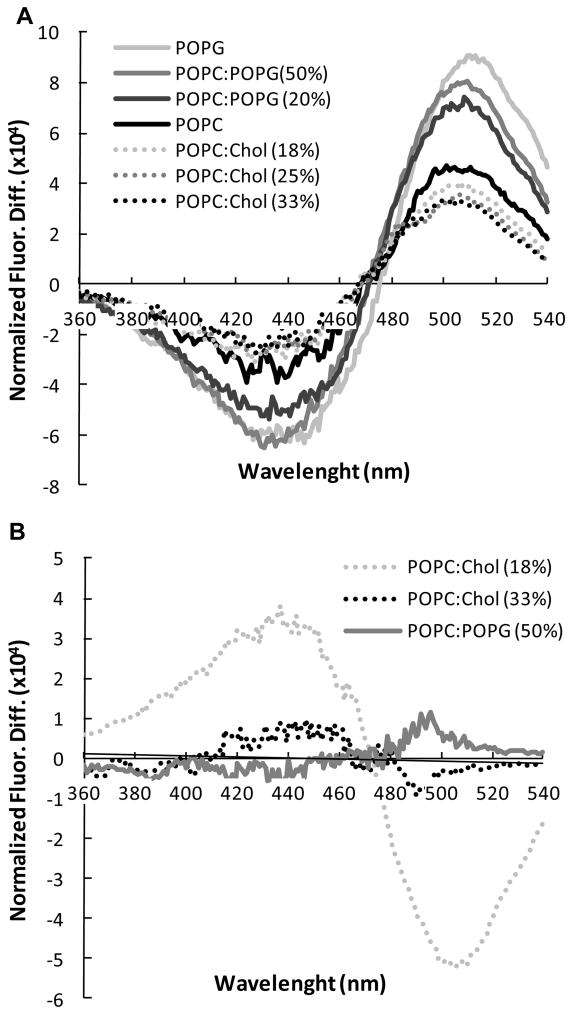

Figure 7. Polarity-sensitive membrane-dependent differential excitation fluorescence spectra of di-8-ANEPPS-labeled vesicles in the presence of IbKTP-NH_2 (A) and morphine (B). Lipid concentration and di-8-ANEPPS were kept constant at 200 μM and 5 μM, respectively. All the assays were performed in 10 mM HEPES buffer pH 7.4, containing NaCl 150 mM. Fluorescence difference spectra were obtained by subtracting the excitation spectrum of di-8-ANEPPS-labeled LUVs in the absence and presence of IbKTP-NH_2 or morphine. Before subtraction, the spectra were normalized to the integrated areas so that the difference spectra reflect only spectral shifts.[42].

appears not to be fundamental for either IbKTP derivative action, contributing to the idea of a membrane as a concentrator of peptide at its surface for receptor binding.[41]

Therefore, lipophilicity correlates to analgesic activity, hypothetically due to (1) a more efficient BBB-translocation process, and/or (2) a membrane-induced optimization of conformation for receptor docking, and/or (3) a simple concentration effect in the vicinity of target receptors.

Two new analgesic compounds were characterized in this study: IbKTP-NH_2 and IbKTP-OH. Synergistic analgesic effects as a result of a concomitant administration of NSAIDs, namely, IBP, and opioids have been reported before.[46] Here, we presented an improved solution: grafting IBP to KTP-NH_2 or KTP-OH resulted in a significantly higher analgesia, when compared with the controls (IBP + KTP-NH_2 or IBP + KTP-OH). It is worth stressing that, in the specific case of IbKTP-OH, the underivatized molecule, KTP, shows no analgesic effect at all when systemically administered, while IbKTP-OH is analgesic. The key difference between them is lipophilicity. This evidence strengthens that hypothesis 1 above may be operative. Mechanistically, ibuprofen seems to function as a carrier, driving KTP through the blood−brain barrier to the target site, the brain.

Reduction in the nociceptive activation of spinal neurons as a result of IbKTP-NH_2 administration provided evidence of central consequences of the analgesic action of the new drug. Curiously, the effects were more pronounced in the inhibition of the deep dorsal horn, which harbors mainly wide dynamic range neurons and is the site of termination of Aβ fibers.[47] Descending modulation from the main pain control center in the brain (the periaqueductal gray PAG) also targets mainly deep dorsal horn neurons, which might be an additional indication of central actions of IbKTP-NH_2. On the other hand, even with naloxone, the IbKTP-NH_2 analgesic effect was still significant, although reduced. Possibly, IbKTP-NH_2 analgesic action may be through two distinct mechanisms: opioid-dependent (prone to be inhibited by naloxone) and opioid-independent. Moreover, a combination of a central and a peripheral effect is likely to occur. This multitarget mechanism of action justifies IbKTP-NH_2 higher analgesic potential.

Unlike morphine, these peptides do not show a preference for cholesterol-rich domains. Furthermore, IbKTP-NH_2 and morphine affect differently the membrane dipole potential. Opioid pathways are involved to some extent, but, in light of these data, IbKTP-NH_2 and morphine do not share the same mechanism of action. Taking together, these new data suggest that, by avoiding the typical opioid-like mechanism of action, the narcotic side effects associated with them might as well be reduced.

■ ASSOCIATED CONTENT

Supporting Information. Localization of peptides in lipid bilayers, additional figures and tables: ^{1}H NMR spectra of compounds **2**, **3** and **5**; biophysical characterization of IbKTP derivatives in aqueous solution and parameters obtained for the partition and quenching of the fluorescence of KTP-NH_2. Additional experimental details: detailed synthesis of IbKTP derivatives, aqueous characterization of compounds, BCEC preparation, animals, acute and inflammatory pain experiments and immunostaining for Fos. This material is available free of charge via the Internet at http://pubs.acs.org.

■ AUTHOR INFORMATION

Corresponding Author

*Faculdade de Medicina de Lisboa, Instituto de Medicina Molecular, Av. Professor Egas Moniz, 1649-028 Lisboa, Portugal. E-mail: macastanho@fm.ul.pt. Tel: (+351) 217 985 136. Fax: (+351) 217 999 477.

■ ACKNOWLEDGMENT

Fundação para a Ciência e Tecnologia (Portugal) is acknowledged for funding (SFRH/BD/42158/2007 fellowship to M.M.B.R., SFRH/BD/41750/2007 fellowship to M.D., SFRH/BPD/37998/2007 fellowship to I.S. and project PTDC/SAU-FCF/69493/2006). Marie Curie Industry-Academia Partnerships and Pathways (European Commission) is also acknowledged for funding (FP7-PEOPLE-2007-3-1-IAPP, Project 230654).

Dra. Susana C. Santos (Instituto de Medicina Molecular, Portugal) is acknowledged for kindly providing HUVEC.

■ ABBREVIATIONS USED

KTP, kyotorphin (Tyr-Arg); KTP-NH_2, kyotorphin amide; IbKTP-NH_2, kyotorphin amide linked to ibuprofen; IbKTP-OH, kyotorphin linked to ibuprofen; IBP, ibuprofen; BBB, blood−brain barrier; BOP, benzotriazol-1-yloxytris(dimethylamino)phosphonium hexafluorophosphate; NMM, *N*-methylmorpholine; DMSO, dimethyl sulfoxide; NMR, nuclear magnetic resonance; DCC, dicyclohexylcarbodiimide; HOBt, *N*-hydroxybenzotriazole; TFA, trifluoroacetic acid; ϕ, fluorescence quantum yield; K_{SV}, Stern−Volmer constant; POPC, 1-palmitoyl-2-oleoyl-*sn*-glycero-3-phosphocholine; POPG, 1-palmitoyl-2-oleoyl-*sn*-glycero-3-(phospho-*rac*-(1-glycerol)); Chol, cholesterol; K_p, partition constant; X_L, fraction of peptide partitioned to the membrane; 5-NS, 5-doxylstearic acid; 16-NS, 16-doxylstearic acid; f_B, fraction of fluorophore accessible to the quencher; f_L, fraction of fluorescence intensity originating from the peptide in the lipid; ip, intraperitoneal; bw, body weight; di-8-ANEPPS, 4-[2-[6-(dioctylamino)-2-naphthalenyl]ethenyl]-1-(3-sulfopropyl)pyridinium; PAG, periaqueductal gray; NSAID, nonsteroidal anti-inflammatory drug; TMA-DPH, trimethylammonium-diphenylhexatriene; ζ, zeta-potential; HPLC, high performance liquid chromatography; HRMS, high resolution mass spectrometry; DMF, *N*,*N*-dimethylformamide; dr, diastereoisomeric ratio; ESI, electrospray ionization; rt, room temperature; TLC:, thin layer chromatography; HEPES, 4-(2-hydroxyethyl)-1-piperazineethanesulfonic acid; i.t., intrathecal; sc, subcutaneous; PBS, phosphate buffer saline; I_W, limit fluorescence intensity in aqueous medium; I_L, limit fluorescence intensity in lipid; γ_L, molar volume of the lipid

■ REFERENCES

(1) Takagi, H.; Shiomi, H.; Ueda, H.; Amano, H. A novel analgesic dipeptide from bovine brain is a possible Met-enkephalin releaser. *Nature* **1979**, *282*, 410–2.

(2) Nishimura, K.; Kaya, K.; Hazato, T.; Ueda, H.; Satoh, M.; Takagi, H. [Kyotorphin like substance in human cerebrospinal fluid of patients with persistent pain]. *Masui* **1991**, *40*, 1686–90.

(3) Shiomi, H.; Ueda, H.; Takagi, H. Isolation and identification of an analgesic opioid dipeptide kyotorphin (Tyr-Arg) from bovine brain. *Neuropharmacology* **1981**, *20*, 633–8.

(4) Ignat'ev, D. A.; Vorob'ev, V. V.; Ziganshin, R. Effects of a number of short peptides isolated from the brain of the hibernating ground squirrel on the EEG and behavior in rats. *Neurosci. Behav. Physiol.* **1998**, *28*, 158–66.

(5) Godlevsky, L. S.; Shandra, A. A.; Mikhaleva, I. I.; Vastyanov, R. S.; Mazarati, A. M. Seizure-protecting effects of kyotorphin and related peptides in an animal model of epilepsy. *Brain Res. Bull.* **1995**, *37*, 223–6.

(6) Chen, P.; Bodor, N.; Wu, W. M.; Prokai, L. Strategies to target kyotorphin analogues to the brain. *J. Med. Chem.* **1998**, *41*, 3773–81.

(7) Lopes, S. C.; Soares, C. M.; Baptista, A. M.; Goormaghtigh, E.; Cabral, B. J.; Castanho, M. A. Conformational and orientational guidance of the analgesic dipeptide kyotorphin induced by lipidic membranes: putative correlation toward receptor docking. *J. Phys. Chem. B* **2006**, *110*, 3385–94.

(8) Lopes, S. C.; Fedorov, A.; Castanho, M. A. Chiral recognition of D-kyotorphin by lipidic membranes: relevance toward improved analgesic efficiency. *ChemMedChem* **2006**, *1*, 723–8.

(9) Ribeiro, M.; Pinto, A.; Pinto, M.; Heras, M.; Martins, I.; Correia, A.; Bardaji, E.; Tavares, I.; Castanho, M. Inhibition of nociceptive responses after systemic administration of amidated kyotorphin. *Br. J. Pharmacol.*

(10) Woodcock, J.; Witter, J.; Dionne, R. A. Stimulating the development of mechanism-based, individualized pain therapies. *Nat. Rev. Drug Discovery* **2007**, *6*, 703–10.

(11) Di Marzo, V.; Bisogno, T.; De Petrocellis, L. Endocannabinoids and related compounds: walking back and forth between plant natural products and animal physiology. *Chem. Biol.* **2007**, *14*, 741–56.

(12) Prins, L. H.; du Preez, J. L.; van Dyk, S.; Malan, S. F. Polycyclic cage structures as carrier molecules for neuroprotective non-steroidal anti-inflammatory drugs. *Eur. J. Med. Chem.* **2009**, *44*, 2577–82.

(13) Mannila, A.; Rautio, J.; Lehtonen, M.; Jarvinen, T.; Savolainen, J. Inefficient central nervous system delivery limits the use of ibuprofen in neurodegenerative diseases. *Eur. J. Pharm. Sci.* **2005**, *24*, 101–5.

(14) Gao, X.; Chen, H.; Schwarzschild, M. A.; Ascherio, A. Use of ibuprofen and risk of Parkinson disease. *Neurology* **2011**, *76*, 863–9.

(15) Santos, N. C.; Castanho, M. Fluorescence spectroscopy methodologies on the study of proteins and peptides. On the 150th anniversary of protein fluorescence. *Trends Appl. Spectrosc.* **2002**, *4*, 113–125.

(16) Mayer, L. D.; Hope, M. J.; Cullis, P. R. Vesicles of variable sizes produced by a rapid extrusion procedure. *Biochim. Biophys. Acta* **1986**, *858*, 161–8.

(17) Santos, N. C.; Prieto, M.; Castanho, M. A. Quantifying molecular partition into model systems of biomembranes: an emphasis on optical spectroscopic methods. *Biochim. Biophys. Acta* **2003**, *1612*, 123–35.

(18) Henriques, S. T.; Castanho, M. A. Environmental factors that enhance the action of the cell penetrating peptide pep-1 A spectroscopic study using lipidic vesicles. *Biochim. Biophys. Acta* **2005**, *1669*, 75–86.

(19) Castanho, M. A.; Prieto, M. J. Fluorescence quenching data interpretation in biological systems. The use of microscopic models for data analysis and interpretation of complex systems. *Biochim. Biophys. Acta* **1998**, *1373*, 1–16.

(20) Fernandes, M. X.; Garcia de la Torre, J.; Castanho, M. A. Joint determination by Brownian dynamics and fluorescence quenching of the in-depth location profile of biomolecules in membranes. *Anal. Biochem.* **2002**, *307*, 1–12.

(21) Matos, P. M.; Goncalves, S.; Santos, N. C. Interaction of peptides with biomembranes assessed by potential-sensitive fluorescent probes. *J. Pept. Sci.* **2008**, *14*, 407–15.

(22) Domingues, M. M.; Castanho, M. A.; Santos, N. C. rBPI(21) promotes lipopolysaccharide aggregation and exerts its antimicrobial effects by (hemi)fusion of PG-containing membranes. *PLoS One* **2009**, *4*, e8385.

(23) Domingues, M. M.; Santiago, P. S.; Castanho, M. A.; Santos, N. C. What can light scattering spectroscopy do for membrane-active peptide studies? *J. Pept. Sci.* **2008**, *14*, 394–400.

(24) Zimmermann, M. Ethical guidelines for investigations of experimental pain in conscious animals. *Pain* **1983**, *16*, 109–10.

(25) Tjolsen, A.; Berge, O. G.; Hunskaar, S.; Rosland, J. H.; Hole, K. The formalin test: an evaluation of the method. *Pain* **1992**, *51*, 5–17.

(26) Coggeshall, R. E. Fos, nociception and the dorsal horn. *Prog. Neurobiol.* **2005**, *77*, 299–352.

(27) Amblard, M.; Rodriguez, M.; Lignon, M. F.; Galas, M. C.; Bernad, N.; Artis-Noel, A. M.; Hauad, L.; Laur, J.; Califano, J. C.; Aumelas, A.; et al. Synthesis and biological evaluation of cholecystokinin analogs in which the Asp-Phe-NH2 moiety has been replaced by a 3-amino-7-phenylheptanoic acid or a 3-amino-6-(phenyloxy)hexanoic acid. *J. Med. Chem.* **1993**, *36*, 3021–8.

(28) Nazare, M.; Waldmann, H. Enantiospecific synthesis of the (9S,18R)-diastereomer of the leukocyte adhesion inhibitor cyclamenol A. *Chem.—Eur. J.* **2001**, *7*, 3363–76.

(29) Konig, W.; Geiger, R. A New Method for Synthesis of Peptides - Activation of Carboxyl Group with Dicyclohexylcarbodiimide Using 1-Hydroxybenzotriazoles as Additives. *Chem. Ber.* **1970**, *103*, 788.

(30) Steinauer, R.; Chen, F. M. F.; Benoiton, N. L. Studies on Racemization Associated with the Use of Benzotriazol-1-yl-tris(dimethylamino)phosphonium hexafluorophosphate (Bop). *Int. J. Pept. Protein Res.* **1989**, *34*, 295–298.

(31) Lakowicz, J. R. *Principles of Fluorescence Spectroscopy*, 2nd ed.; Kluwer Academic/Plenum Publishers: New York, 1999.

(32) Ross, J. B. A.; Laws, W. R.; Rousslang, K. W.; Wyssbrod, H. R. Tyrosine fluorescence and phosphorescence from proteins and polypeptides. In *Topics in Fluorescence Spectroscopy, Vol. 3: Biochemical Applications*; Lakowicz, J. R., Ed.; Plenum Press: New York, 1992; pp 1−63.

(33) Mrozek, J.; Rzeska, A.; Guzow, K.; Karolczak, J.; Wiczk, W. Influence of alkyl group on amide nitrogen atom on fluorescence quenching of tyrosine amide and N-acetyltyrosine amide. *Biophys. Chem.* **2004**, *111*, 105–13.

(34) Reyes Mateo, C.; Ulises Acuna, A.; Brochon, J. C. Liquid-crystalline phases of cholesterol/lipid bilayers as revealed by the fluorescence of trans-parinaric acid. *Biophys. J.* **1995**, *68*, 978–87.

(35) Goldenberg, N. M.; Steinberg, B. E. Surface charge: a key determinant of protein localization and function. *Cancer Res.* **2010**, *70*, 1277–80.

(36) Bars, D. l.; Gozariu, M.; Cadden, S. W. Animal Models of Nociception. *Pharmacol. Rev.* **2001**, *53*, 597–652.

(37) Dubuisson, D.; Dennis, S. G. The formalin test: a quantitative study of the analgesic effects of morphine, meperidine, and brain stem stimulation in rats and cats. *Pain* **1977**, *4*, 161–74.

(38) Rackham, A.; Wood, P. L.; Hudgin, R. L. Kyotorphin (tyrosine-arginine): further evidence for indirect opiate receptor activation. *Life Sci.* **1982**, *30*, 1337–42.

(39) Huidobro-Toro, J. P.; Canessa, M.; Fischer, S. Interaction of morphine with cholesterol monolayers. *Biochim. Biophys. Acta* **1976**, *436*, 237–41.

(40) Cladera, J.; Martin, I.; O'Shea, P. The fusion domain of HIV gp41 interacts specifically with heparan sulfate on the T-lymphocyte cell surface. *EMBO J.* **2001**, *20*, 19–26.

(41) Castanho, M. A.; Fernandes, M. X. Lipid membrane-induced optimization for ligand-receptor docking: recent tools and insights for the "membrane catalysis" model. *Eur. Biophys. J.* **2006**, *35*, 92–103.

(42) Veiga, S.; Yuan, Y.; Li, X.; Santos, N. C.; Liu, G.; Castanho, M. A. Why are HIV-1 fusion inhibitors not effective against SARS-CoV? Biophysical evaluation of molecular interactions. *Biochim. Biophys. Acta* **2006**, *1760*, 55–61.

(43) Romanowski, M.; Zhu, X. Y.; Kim, K.; Hruby, V. J.; O'Brien, D. F. Interaction of enkephalin peptides with anionic model membranes. *Biochim. Biophys. Acta, Biomembr.* **2002**, *1558*, 45–53.

(44) Tamai, I.; Sai, Y.; Kobayashi, H.; Kamata, M.; Wakamiya, T.; Tsuji, A. Structure-internalization relationship for adsorptive-mediated endocytosis of basic peptides at the blood-brain barrier. *J. Pharmacol. Exp. Ther.* **1997**, *280*, 410–5.

(45) Yeung, T.; Gilbert, G. E.; Shi, J.; Silvius, J.; Kapus, A.; Grinstein, S. Membrane phosphatidylserine regulates surface charge and protein localization. *Science* **2008**, *319*, 210–3.

(46) Kolesnikov, Y.; Soritsa, D. Analgesic synergy between topical opioids and topical non-steroidal anti-inflammatory drugs in the mouse model of thermal pain. *Eur. J. Pharmacol.* **2008**, *579*, 126–33.

(47) Morris, R.; Cheunsuang, O.; Stewart, A.; Maxwell, D. Spinal dorsal horn neurone targets for nociceptive primary afferents: do single neurone morphological characteristics suggest how nociceptive information is processed at the spinal level. *Brain Res. Brain Res. Rev.* **2004**, *46*, 173–90.